nature cell biology

Mechanosensitive gating of CFTR

Wei Kevin Zhang[1,2,6], Dong Wang[2,5,6], Yuanyuan Duan[2], Michael M.T. Loy[1,3], Hsiao Chang Chan[4] and Pingbo Huang[1,2,7]

Cystic fibrosis transmembrane conductance regulator (CFTR) is an anion and intracellular ligand-gated channel associated with cystic fibrosis, a lethal genetic disorder common among Caucasians[1]. Here we show that CFTR is robustly activated by membrane stretch induced by negative pressures as small as 5 mmHg at the single-channel, cellular and tissue levels. Stretch increased the product of the number of channels present and probability of being open (NPo), and also increased the unitary conductance of CFTR in cell-attached membrane patches. CFTR stretch-mediated activation appears to be an intrinsic property independent of cytosolic factors and kinase signalling. CFTR stretch-mediated activation resulted in chloride transport in Calu-3 human airway epithelial cells and mouse intestinal tissues. Our study has revealed an unexpected function of CFTR in mechanosensing, in addition to its roles as a ligand-gated anion channel[1] and a regulator of other membrane transporters[2], demonstrating for the first time a mechanosensitive anion channel with a clearly defined molecular identity. Given that CFTR is often found in mechanically dynamic environments, its mechanosensitivity has important physiological implications in epithelial ion transport and cell volume regulation *in vivo*.

In a quiescent cell-attached membrane patch of Calu-3 human airway epithelial cells known to express CFTR (ref. 3), application of negative pressure or suction of 15 mmHg to the back of the pipette activated a channel with slow kinetics and a unitary conductance of ~6–7 pS at a pipette potential (Vp) of –60 mV (I in Fig. 1a), the same channel characteristics shown by the cAMP-activated CFTR channel in the same patch (V in Fig. 1a)[3,4]. In 19 (61%) of 31 cell-attached patches that showed stretch-activated channel activity following suctions of up to 60 mmHg, further challenge with a cAMP 'cocktail' (see Methods) activated the CFTR channel. These data suggest that stretch and cAMP may both activate CFTR. Given that cAMP cannot consistently activate CFTR in cell-attached patches[3,5], the lower frequency of observing cAMP-mediated activation of CFTR than its stretch-mediated activation is expected. The stretch-mediated activation was greatly attenuated in the presence of cAMP, which strongly activated CFTR (Supplementary Fig. 1), implying that suction- and cAMP-activated single-channel currents are mediated by a common ion channel, that is, CFTR, rather than by two independent ion channels. Alternatively, as CFTR regulates other ion transporters and channels[2], this result may suggest that CFTR cAMP-mediated activation inhibits the presumed stretch-activated channel, but such a suggestion is inconsistent with the observation that blocking CFTR by the CFTR-specific blocker GlyH-101 also blocked the stretch-activated channel (Fig. 1b). Moreover, the stretch-activated channel showed burst-like openings and strong flickering kinetics at a positive pipette potential, a signature of cAMP-activated CFTR channels (Supplementary Fig. 2)[3,5–7].

CFTR NPo was activated by mild suction of 15 mmHg and plateaued at 45 mmHg at –60 mV Vp (I–IV in Fig. 1a, Fig. 1c, and Supplementary Fig. 3). CFTR activation occurred within 2 s after stretch and immediately reached a sustained maximal activation (I–IV in Fig. 1a, I in Fig. 1b, and Fig. 1d). The stretch-mediated activation onset was accelerated with increasing negative pressures (I–IV in Fig. 1a and Fig. 1d). The onset delay may at least partially reflect the time required to develop pressure within the membrane or the cell. The abrupt onset and maximization of channel activation seem to suggest that the channel is activated either by mechanical force directly or by mechanosensitive second messengers with extremely fast turn-on times. Protein kinases A and C (PKA and PKC), which are known to activate CFTR, did not seem to mediate CFTR stretch-mediated activation, because their blockers had no effect on the stretch-mediated activation (Supplementary Fig. 4). Ca^{2+} was also not involved, as the stretch-mediated activation was observed without extracellular Ca^{2+} ($n = 3$) or with BAPTA-AM ($n = 4$), an intracellular Ca^{2+} chelator (data not shown).

Interestingly, membrane stretch also altered CFTR unitary conductance, as has been previously observed in other stretch-activated channels[8,9]. At –60 mV Vp, the CFTR channel current amplitude activated by 15 mmHg suction (I in Fig. 1a), which was almost indistinguishable from that activated by cAMP (V in Fig. 1a), was slightly increased by

[1]Nano Science and Technology Program, [2]Department of Biology and [3]Department of Physics, The Hong Kong University of Science and Technology, Hong Kong SAR, People's Republic of China and [4]Epithelial Cell Biology Research Center, Key Laboratory for Regenerative Medicine of Ministry of Education of China, School of Biomedical Sciences, Faculty of Medicine, The Chinese University of Hong Kong, Hong Kong SAR, People's Republic of China.
[5]Current address: Department of Molecular and Cellular Physiology, School of Medicine, Stanford University, Stanford CA 94305, USA.
[6]These authors contributed equally to this work.
[7]Correspondence should be addressed to P.H. (e-mail: bohuangp@ust.hk)

Received 14 December 2009; accepted 9 March 2010; published online 18 April 2010; DOI: 10.1038/ncb2053

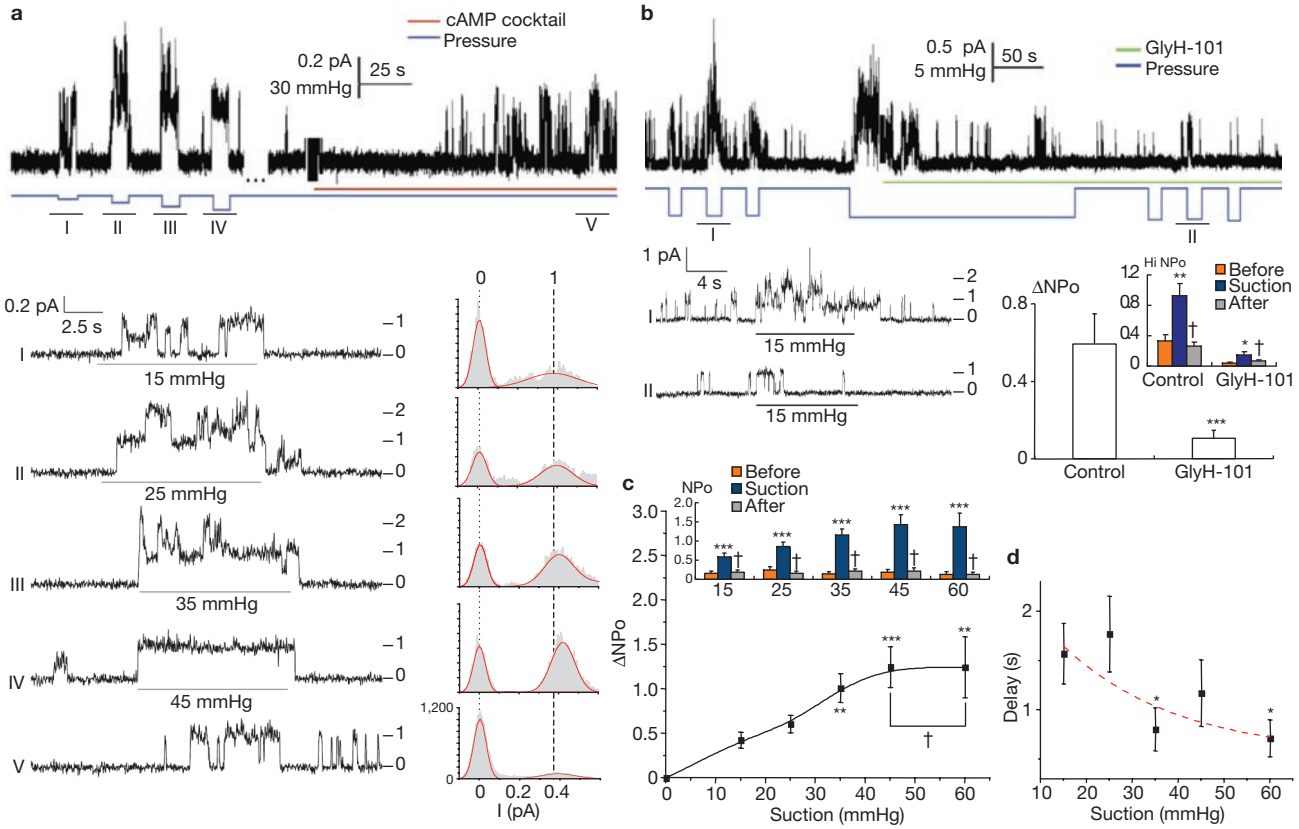

Figure 1 Stretch increased CFTR NPo in cell-attached membrane patches of Calu-3 cells. (**a**) Upper: CFTR in response to suction and cAMP. Dotted line, recording omitted for clarity. Lower: time-expansion of segments I–V and corresponding all-points amplitude histograms of the first-level channel. Numbers and dashes, the active channel number; red curves, the Gaussian fitting. (**b**) Upper: CFTR stretch-activation before and after 40 μM GlyH-101 at –100 mV Vp. Lower: time-expansion of segments I–II and summary data of NPo change (ΔNPo) in response to suction of 15 mmHg before and after GlyH-101. ***, different from before GlyH-101, $P = 0.00013$. ΔNPo in **b** and **c** is the difference between NPo during (10 s) and average NPo of before (10 s) and after (10 s) suction (insets). Inset: **, different from before suction, $P = 0.0036$; *, $P = 0.022$ †, $P \geq 0.18$; data are mean ± s.e.m. of 6 patches. (**c**) ΔNPo in response to different negative pressures at –60 mV Vp. ***, different from 15 mmHg, $P = 0.00042$; **, $P \leq 0.0063$; †, $P = 0.90$. Inset: ***, different from before suction, $P \leq 0.00093$; †, $P \geq 0.15$. Data are mean ± s.e.m. of $n = 54$ (15 mmHg), 54 (25 mmHg), 54 (35 mmHg), 41 (45 mmHg) and 36 (60 mmHg) patches. (**d**) Onset delay of the stretch-activation. The delay is calculated from the recordings without basal channel activity in the 10 s before suction. *, different from 15 mmHg, $P \leq 0.043$; data are mean ± s.e.m. of $n = 40$ (15 mmHg), 40 (25 mmHg), 40 (35 mmHg), 38 (45 mmHg) and 32 (60 mmHg) patches; dotted line, exponential fit.

a higher pressure; this increase was most evident at 45 mmHg (I–IV in Fig. 1a). The current amplitude increase did not result from a transient change in the seal resistance or the cell membrane potential, because the same pressure failed to generate any transient current in quiescent membrane patches (data not shown). The stretch-induced current amplitude change at –60 mV Vp increased with increasing suction up to 45 mmHg (Fig. 2a). Consistent with the idea that the stretch-activated channel is CFTR, extrapolation of a linear regression of the channel current amplitudes between 15 and 45 mmHg suggests that the theoretical channel current amplitude at 0 mmHg is 0.410 ± 0.017 pA, identical to that of cAMP-activated CFTR single channels (0.410 ± 0.020 pA, $n = 19$). The change in stretch-induced current amplitude in the same channel was further demonstrated by application of ramp suction (Fig. 2b, c). At –60 mV Vp, membrane stretch increased the single-channel current amplitude by as much as 30% (Fig. 2a). Similar observations were also obtained at different pipette potentials (Supplementary Fig. 2 and Fig. 2d). The current–voltage (IV) relation of the stretch-activated CFTR channels at 35 mmHg resembles that of cAMP-activated CFTR, with much smaller amplitudes at positive pipette potentials, which presumably results from a lower intracellular Cl^- concentration[5,7]. These data indicate that membrane stretch increases CFTR unitary conductance in addition to its NPo.

CFTR mechanosensitivity was next examined in excised, inside-out membrane patches. Because PKA and other signalling molecules are retained in excised membrane patches of Calu-3 cells[4,10,11], the experiments were carried out in the absence of ATP, a substrate indispensable for the activities of all kinases, in order to rule out possible involvement of any kinases. CFTR opens with a low probability without ATP, although ATP binding and hydrolysis control the CFTR channel gating and increase the opening rate[12,13]. Stretch activated CFTR in excised, inside-out patches without ATP (Fig. 3a, b), suggesting that ATP (and therefore all kinases) and other cytosolic factors may not be essential to the stretch-mediated activation and that CFTR is probably a direct mechanosensitive channel. CFTR stretch-mediated activation reduced by ~60% following excision (Fig. 3a, b), indicating that an unknown cytosolic factor(s) or cytoskeletal integrity, although not essential, may positively modulate CFTR mechanosensitivity. In line with the notion

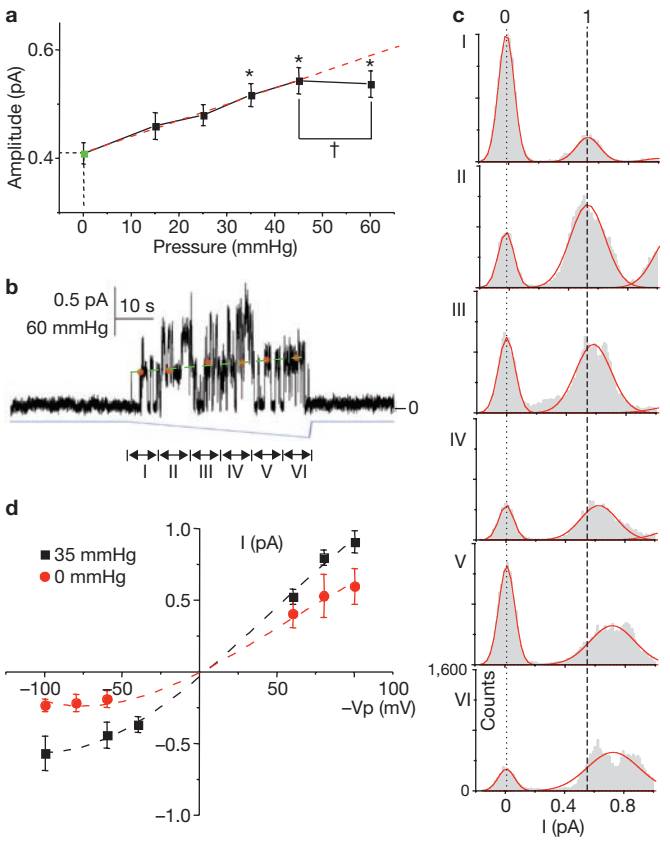

Figure 2 Membrane stretch increased CFTR single-channel current amplitude in cell-attached membrane patches of Calu-3 cells. (**a**) Summary data of the single-channel current amplitude of CFTR in response to suction steps at –60 mV Vp. Data are mean ± s.e.m. of $n = 30$ (15 mmHg), 40 (25 mmHg), 35 (35 mmHg), 25 (45 mmHg) and 16 (60 mmHg) patches. *, different from amplitude at 15 mmHg, $P \leq 0.040$; †, $P = 0.86$. The data point in green is the single-channel current amplitude of cAMP-activated CFTR at –60 mV Vp ($n = 19$ patches; mean ± s.e.m.). (**b**) The current amplitude of CFTR in a cell-attached membrane patch in response to a ramp pressure application at –60 mV Vp; one of three similar experiments is shown. The red dots represent the average current amplitudes of the first-level channel in segments I–VI, which are calculated from the corresponding all-points amplitude histograms in (**c**). The red dots elevated with increasing negative pressures. (**d**) Current–voltage (IV) relationships of CFTR activated by cAMP (red; data are mean ± s.e.m. of $n = 6$ (+100 mV), 6 (+80 mV), 11 (+60 mV), 6 (–60 mV), 6 (–80 mV) and 7 (–100 mV) patches) or suction of 35 mmHg (black; data are mean ± s.e.m. of $n = 6$ (+100 mV), 6 (+80 mV), 8 (+60 mV), –8 (–40 mV), 7 (–60 mV) and 8 (–100 mV) patches).

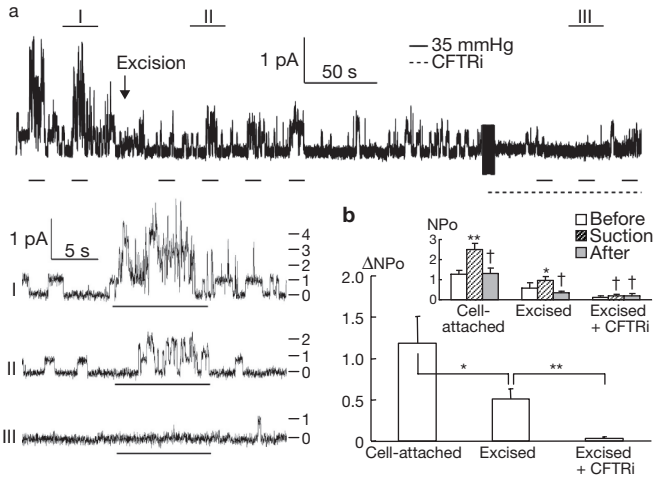

Figure 3 Stretch increased CFTR NPo in excised, inside-out membrane patches of Calu-3 cells in the absence of ATP. (**a**) Upper: CFTR stretch-activation before and after membrane excision and 20 μM CFTRinh-172 at –60 mV Vp. Lower: time-expansion of segments I–III. Numbers and dashes indicate the number of active channels. (**b**) Summary data of ΔNPo in response to suction of 35 mmHg before and after membrane excision and CFTRinh-172. *, $P = 0.031$; **, $P = 0.0021$. ΔNPo is the difference between NPo during (10 s) and average NPo of before (10 s) and after (10 s) suction (insets). Inset: **, different from before suction, $P = 0.0082$; *, $P = 0.031$; †, $P \geq 0.38$; data are mean ± s.e.m. of $n = 8$ patches.

that CFTR underlies the stretch-activated currents, the stretch-activated channel was blocked by a CFTR-specific inhibitor, CFTRinh-172 (CFTRi) (Fig. 3a, b). Also, the stretch-activated channel seems to be anion-selective, because without permeable cation in the pipette it was conductive, and its single-channel conductance remained almost the same at a negative Vp following membrane excision (excision removed any permeable cations on the cytosolic side) (Fig. 3a).

Although patch-clamp techniques are powerful for dissecting mechanosensitive channels in membrane patches, the process of forming a giga-seal (a tight seal with giga-ohm electrical resistance) may traumatize membrane patches and alter their native mechanical state and the behaviour of resident channels[14-16]. To examine the stretch-mediated activation of CFTR *in situ* and its physiological relevance, CFTR mechanosensitivity was examined in Calu-3 epithelial monolayers, with Ussing chambers adapted for pressure applications. Under conditions for measuring the short-circuit current (I_{sc}), which is a complex readout of several ion channels and transporters, including CFTR, an apical suction of 10 mmHg or 50 mmHg elicited a change in I_{sc} (ΔI_{sc}), which was suppressed by ~33–57% by CFTRi, glybenclamide and GlyH-101 (Fig. 4a, b). Similar blocker sensitivities were observed for cAMP-induced, CFTR-mediated ΔI_{sc} (~36–55% inhibition, Fig. 4c, d), indicating that suction-activated ΔI_{sc} is mostly, if not all, mediated by CFTR. Interestingly, CFTR inhibitors caused considerably less inhibition of stretch-induced transepithelial conductance change (ΔG_{te}, ~7–18% inhibition) than on the corresponding ΔI_{sc} with both 10 mmHg and 50 mmHg suctions (Fig. 4a, b). One possibility is that stretch induced a paracellular conductance or permeability (G_{shunt}) increase[17,18] that contributed more than 50% of stretch-induced ΔG_{te}. A change in G_{shunt} contributes very little, if anything at all, to I_{sc}, especially with fluid resistance compensation in our experiments. This means that stretch-induced ΔI_{sc}, which is predominantly dictated by transcellular conductance (G_c, that is, CFTR) and independent of G_{shunt}, would not correlate with a ΔG_{te}, which largely reflects G_{shunt} change. Another possibility is that the reduction in G_c (that is, in conductance through CFTR) that is directly caused by CFTR inhibitors is cancelled out by a G_{te} increase secondary to suppression of CFTR-mediated anion secretion and the resulting 'collapse' of the lateral intercellular space[19,20].

To rule out the contributions of other mechanosensitive channels to the I_{sc}, the stretch response of an apical CFTR-mediated Cl^- current (I_{Cl}) in isolation was assessed by using basolaterally permeabilized Calu-3 monolayers. The apical suction activated ΔI_{Cl}, which was blocked by ~65–75% by CFTR inhibitors (Fig. 4e–g), similar to cAMP-activated, CFTR-mediated ΔI_{Cl} (Fig. 4h–i, ~40–53% inhibition). In contrast, both currents were virtually unresponsive to 4,4′-diisothiocyanatostilbene-2,2′-disulfonic acid

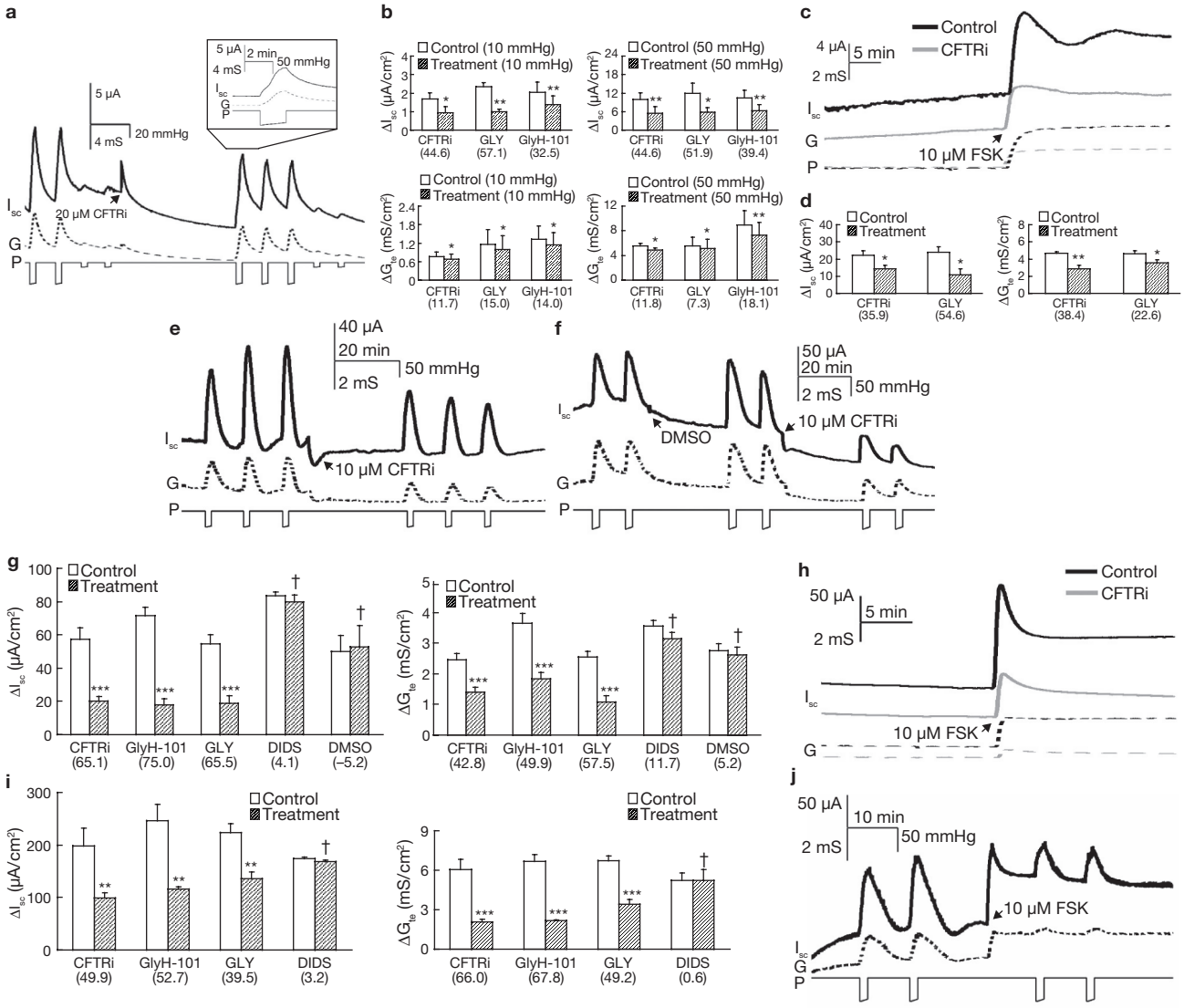

Figure 4 Membrane stretch stimulated CFTR-mediated anion secretion in Calu-3 cells. (**a**) Stretch-activated ΔI_{sc} and corresponding ΔG_{te} before and after 20 µM CFTRi. G, transepithelial conductance G_{te}; P, pressure. The pressure was released at the response plateau in all the experiments (inset). The slight decline in the pressure pulse was presumably a result of inherently imperfect sealing of the agar salt bridge connections in the Ussing chambers. (**b**) Summary data of **a** ($n = 5$) and similar experiments with 300 µM glybenclamide (GLY, $n = 5$) or 40 µM GlyH-101 ($n = 9$). *n*, number of independent experiments, each with duplicate or triplicate stretches; **, different from control, $P \leq 0.0094$; *, $P \leq 0.041$; number in parentheses in **b** and following panels, percentage of inhibition. (**c**) cAMP-activated ΔI_{sc} and corresponding ΔG_{te} with and without 20 µM CFTRi. FSK, forskolin. (**d**) Summary data of **c** ($n = 5$) and similar experiments with 300 µM glybenclamide ($n = 5$). **, different from control, $P \leq 0.0032$; *, different from control, $P \leq 0.048$. (**e**, **f**) Stretch-activated apical ΔI_{Cl} and corresponding ΔG_{te} before and after 10 µM CFTRi (**e**) or vehicle (DMSO, **f**). (**g**) Summary data of **e** ($n = 7$), similar experiments with GlyH-101 (40 µM, $n = 6$), glybenclamide (300 µM, $n = 5$) and DIDS (100 µM, $n = 4$), and **f** ($n = 5$). ***, different from control, $P \leq 0.00038$; †, $P \geq 0.18$. (**h**) cAMP-activated ΔI_{Cl} and corresponding ΔG_{te} with and without 10 µM CFTRi. (**i**) Summary data of **h** ($n = 8$) and similar experiments with GlyH-101 (40 µM, $n = 6$), glybenclamide (300 µM, $n = 6$) and DIDS (100 µM, $n = 3$). **, different from control, $P \leq 0.01$; ***, different from control, $P \leq 0.00013$; †, $P \geq 0.34$. (**j**) Stretch-activated apical ΔI_{Cl} and corresponding ΔG_{te} before and after 10 µM forskolin. All data are mean ± s.e.m.

(DIDS) or the vehicle (Fig. 4f, g). These data suggest that suction-activated ΔI_{Cl} is mostly, if not all, mediated by CFTR, instead of by a DIDS-sensitive, volume-activated chloride channel[21]. Moreover, the stretch response of ΔI_{Cl} was substantially attenuated following CFTR pre-activation by 10 µM forskolin (Fig. 3j; 105.2 ± 9.7 µA per cm^2 before and 53.4 ± 4.8 µA per cm^2 after forskolin, $n = 5$, $P = 0.00028$), agreeing with the results in Supplementary Fig. 1 and reinforcing the idea that suction- and cAMP-activated channel currents share a common chloride channel, that is, CFTR.

The three CFTR inhibitors caused moderately lower inhibition on stretch-induced ΔG_{te} (Fig. 4e–g, ~43–58% inhibition), but greater inhibition on cAMP-induced ΔG_{te} (Fig. 4 h–i, ~49–68% inhibition), than on their corresponding ΔI_{Cl}. These observations argue against the idea that a reduction in G_c (CFTR) directly induced by CFTR inhibitors is cancelled out by a G_{te} increase secondary to suppression of CFTR-mediated anion secretion. Had this occurred, smaller rather than greater inhibition on cAMP-induced ΔG_{te} than on the corresponding ΔI_{Cl} would have been observed. Therefore, the lower level of inhibition of stretch-activated ΔG_{te}

than of corresponding ΔI_{Cl} is likely to be a result of stretch-activated ΔG_{te} containing a G_{shunt} component. This component may not contribute much to ΔI_{Cl}, even with a Cl^- gradient imposed across the epithelia under I_{Cl} conditions, if the paracellular conductance is selectively permeable to Na^+, as previously reported[22]. These results imply that negative pressure, at least 50 mmHg suction, may alter both CFTR and paracellular conductance. Stretch-induced ΔG_{shunt} might result from dilation of lateral intercellular spaces or structural changes in tight junctions[18]. Whether it could facilitate coupling of the passive flow of counter ions to active transcellular transport, thereby governing transepithelial electrolyte and water transport as has been previously suggested, remains to be determined[22].

Moreover, suction did not seem to activate CFTR indirectly by promoting the release of ATP and adenosine, which activate cAMP and Ca^{2+} signalling[23], or by other mechanosensitive PKA or PKC signalling, because suction-activated ΔI_{sc} or ΔI_{Cl} was insensitive to the P2 receptor blocker PPADS, adenosine deaminase (ADA), the adenosine receptor blocker 8-SPT, BAPTA-AM, the adenylate cyclase blocker MDL-12330A, the PKA inhibitor H89 and the PKC inhibitor BIMII (Supplementary Fig. 5a–c), which were all effective in their respective control experiments (data not shown). In addition, the effect of PKA phosphorylation on CFTR mechanosensitivity was assessed, as PKA and PKC phosphorylation modulate the mechanosensitivity of some ion channels[24]. Instead of using 10 μM forskolin, which sub-maximally activated CFTR and attenuated its stretch-mediated response (Fig. 4j), we used 0.01 μM and 0.1 μM forskolin to induce a low-level PKA phosphorylation of CFTR; this low level was indicated by the moderate ΔI_{Cl} seen with these concentrations (Supplementary Fig. 5d, e). However, these concentrations of forskolin had little impact on the CFTR stretch-mediated response induced by 20 mmHg suction (Supplementary Fig. 5d, e), suggesting that cAMP–PKA signalling does not also modulate CFTR mechanosensitivity. Suction of as little as 5 mmHg elicited a significant ΔI_{Cl}, and ΔI_{Cl} increased with increasing apical suction (Supplementary Fig. 6a, b). Unlike some other mechanosensitive channels[25], CFTR stretch-mediated activation showed little adaptation even with a suction for as long as 10 min (Supplementary Fig. 6c).

In the duodenum of *Cftr* wild-type mice, an apical suction activated a ΔI_{sc} that was sensitive to CFTRi (Fig. 5a; 11.5 ± 0.9 μA/cm² before and 5.3 ± 0.5 μA/cm² after CFTRinh-172, $n = 6$, $P = 0.00001$). However, suction- and cAMP-activated ΔI_{sc} were substantially reduced or eliminated in samples obtained from $Cftr^{-/-}$ knockout littermates (Fig. 5b, c). Similarly, the ablation of *Cftr* gene greatly suppressed suction-activated ΔI_{sc} in the jejunum, without any effect on glucose-induced ΔI_{sc}, which is used as a functional test of tissue viability and integrity (Fig. 5d, e)[26, 27]. These observations suggest that CFTR mediates a stretch-activated transepithelial anion transport.

Intriguingly, the ablation of the *Cftr* gene completely eliminated cAMP-activated, but not stretch-activated, ΔI_{sc}, suggesting that an ion channel(s) other than CFTR may contribute to stretch-induced ΔI_{sc}. It is not clear what the molecular identity of the channel is. One possibility is that there is another mechanosensitive chloride conductance in the apical membrane, or a mechanosensitive potassium channel in the basolateral membrane (in this case an apical potassium conductance for supplying potassium would be needed). The residual stretch-activated ΔI_{sc} in $Cftr^{-/-}$ mice is not due to a potential suction-induced ΔG_{shunt}, as ΔG_{shunt} contributes little to I_{sc}.

Our study reveals an unexpected function of CFTR in mechanosensing, in addition to its well-documented roles as a ligand-gated anion channel and as a regulator of other membrane transporters[2]. To our knowledge,

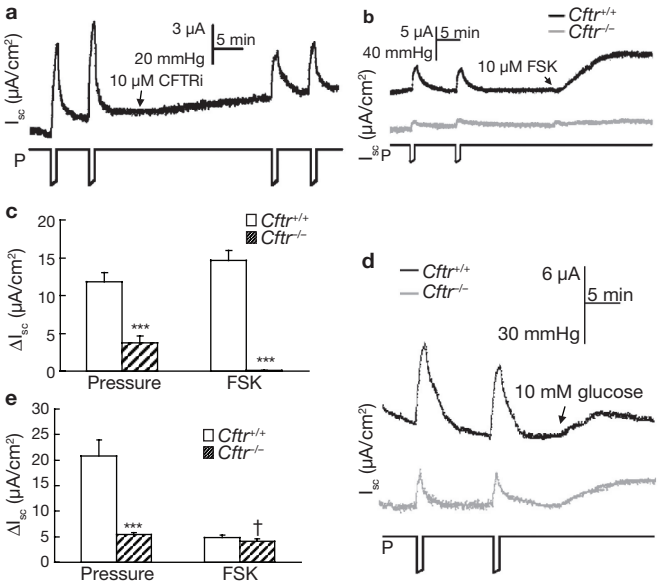

Figure 5 Membrane stretch activated CFTR-mediated anion secretion in mouse intestinal tissues. (**a**) Stretch-activated ΔI_{sc} in the duodenum in a wild-type mouse before and after 10 μM CFTRi treatment. (**b**) Stretch- and cAMP-activated ΔI_{sc} in the duodenum in wild-type and *Cftr* knockout mice. (**c**) Summary data of **b**. $n = 7$ for $Cftr^{+/+}$ and $n = 4$ for $Cftr^{-/-}$ littermates, each with duplicate or triplicate duodenum segments. ***, different from control, $P \leq 0.0013$. (**d**) Stretch- and glucose (10 mM)-activated ΔI_{sc} in the jejunum in wild-type and *Cftr* knockout littermates. (**e**) Summary data of **d**. $n = 5$ for $Cftr^{+/+}$ and $n = 5$ for $Cftr^{-/-}$ littermates, each with duplicate or triplicate jejunum segments. ***, different from control, $P = 0.0001$. †, $P = 0.27$. P in **a, b**, **d**, pressure. All data are mean ± s.e.m.

this study is the first to report a mechanosensitive anion channel with a known molecular identity, contrasting to many reported mechanosensitive cation channels with clear genetic identities[28]. We found that CFTR mechanosensitivity mediates stretch-induced chloride transport in Calu-3 human airway epithelia cells and mouse intestinal tissues.

In many epithelial tissues *in vivo*, especially those in the airways, CFTR is often exposed to a highly mechanically dynamic environment. Although the pressure in an airway at rest is basically normobaric with 3-4 mmHg fluctuation, it becomes very hypobaric during exercise (–30 mmHg)[29], in the pressurized cabins of commercial aircraft (–200 mmHg)[30], and at high altitudes. In addition, the hydrostatic pressure in the submucosal tissue could be significantly elevated in pronounced submucosal oedema in pathological conditions such as asthma[18]. All these situations, on the basis of our findings, would activate CFTR. On the other hand, hypotonicity also generates a considerable mechanical stress on the cell membranes of epithelia, which could stimulate mechanosensitive channels such as CFTR. Although the volume regulation in epithelial cells has been extensively studied, the molecular identity of the underlying chloride channel remains as yet unelucidated[31, 32]. It has been observed that the loss of CFTR impairs the regulatory volume decrease (RVD) of epithelial cells in response to hypotonic challenge[33–35]. It was proposed that CFTR is indirectly involved in RVD, possibly via regulating basolateral calcium-activated potassium channels[35, 36] or ATP release[34, 37] by undefined mechanisms. In view of our finding that stretch activates CFTR, it seems plausible that CFTR might directly mediate RVD in epithelial cells by responding to hypotonicity-induced membrane stress. Given that CFTR is often found in mechanically dynamic environments, such as

the lung, intestine and reproductive tracts, its mechanosensitivity is of great physiological relevance and has important biological implications in these tissues *in vivo*. In addition, because CFTR also regulates other important membrane transporters and ion channels, such as epithelial sodium channels and the outwardly rectified chloride channels, its mechanosensitivity may have a far-reaching impact on our understanding of how other related epithelial membrane transporters and ion channels are controlled by mechanical forces.

METHODS

Methods and any associated references are available in the online version of the paper at http://www.nature.com/naturecellbiology/

Note: Supplementary Information is available on the Nature Cell Biology website.

ACKNOWLEDGEMENTS

We thank R. Madhavan for stimulating discussion, J.M. Stutts for critical reading of the manuscript and Changyan Xie for assistance in manuscript preparation. This work was supported by the Hong Kong Research Grants Council grant GRF661009 (to P.H.).

AUTHOR CONTRIBUTIONS

W.K.Z, D.W. and P.H. conceived the study and P.H. directed the study; W.K.Z performed and analysed most of the patch-clamp work with some help from D.W.; D.W. performed and analysed most of the Ussing chamber work with some help from W.K.Z and D.Y.; M.M.T.L designed the Ussing chamber adapted for pressure applications; H.C.C. provided *Cftr* knockout mice, critical comments and revision of the manuscript; P.H., W.K.Z. and D.W. drafted the manuscript; and P.H. revised the manuscript with contributions from all the authors.

COMPETING FINANCIAL INTEREST

The authors declare no competing financial interests.

Published online at http://www.nature.com/naturecellbiology/
Reprints and permissions information is available online at http://npg.nature.com/reprintsandpermissions/

1. Gadsby, D. C. & Nairn, A. C. Control of CFTR channel gating by phosphorylation and nucleotide hydrolysis. *Physiol. Rev.* **79**, S77–107 (1999).
2. Schwiebert, E. M., Benos, D. J., Egan, M. E., Stutts, M. J. & Guggino, W. B. CFTR is a conductance regulator as well as a chloride channel. *Physiol. Rev.* **79**, S145–166 (1999).
3. Haws, C., Finkbeiner, W. E., Widdicombe, J. H. & Wine, J. J. CFTR in Calu-3 human airway cells: channel properties and role in cAMP-activated Cl- conductance. *Am. J. Physiol.* **266**, L502–512 (1994).
4. Huang, P. *et al.* Compartmentalized autocrine signaling to cystic fibrosis transmembrane conductance regulator at the apical membrane of airway epithelial cells. *Proc. Natl Acad. Sci. USA* **98**, 14120–14125 (2001).
5. Haws, C., Krouse, M. E., Xia, Y., Gruenert, D. C. & Wine, J. J. CFTR channels in immortalized human airway cells. *Am. J. Physiol.* **263**, L692–707 (1992).
6. Fischer, H., Illek, B. & Machen, T. E. Regulation of CFTR by protein phosphatase 2B and protein kinase C. *Pflugers Arch.* **436**, 175–181 (1998).
7. Fischer, H. & Machen, T. E. CFTR displays voltage dependence and two gating modes during stimulation. *J. Gen Physiol.* **104**, 541–566 (1994).
8. Chang, W. & Loretz, C. A. Activation by membrane stretch and depolarization of an epithelial monovalent cation channel from teleost intestine. *J. Exp. Biol.* **169**, 87–104 (1992).
9. Yao, X., Kwan, H. & Huang, Y. Stretch-sensitive switching among different channel sublevels of an endothelial cation channel. *Biochi. Biophys. Acta* **1511**, 381–390 (2001).
10. Barnes, A. P. *et al.* Phosphodiesterase 4D forms a cAMP diffusion barrier at the apical membrane of the airway epithelium. *J. Biol. Chem.* **280**, 7997–8003 (2005).
11. Huang, P., Trotter, K., Boucher, R. C., Milgram, S. L. & Stutts, M. J. PKA holoenzyme is functionally coupled to CFTR by AKAPs. *Am. J. Physiol. Cell Physiol.* **278**, C417–422 (2000).
12. Bompadre, S. G., Li, M. & Hwang, T. C. Mechanism of G551D-CFTR (cystic fibrosis transmembrane conductance regulator) potentiation by a high affinity ATP analog. *J. Biol. Chem.* **283**, 5364–5369 (2008).
13. Hwang, T. C. & Sheppard, D. N. Gating of the CFTR Cl- channel by ATP-driven nucleotide-binding domain dimerisation. *J. Physiol.* **587**, 2151–2161 (2009).
14. Morris, C. E. & Sigurdson, W. J. Stretch-inactivated ion channels coexist with stretch-activated ion channels. *Science* **243**, 807–809 (1989).
15. Wan, X., Juranka, P. & Morris, C. E. Activation of mechanosensitive currents in traumatized membrane. *Am. J. Physiol.* **276**, C318–327 (1999).
16. Small, D. L. & Morris, C. E. Delayed activation of single mechanosensitive channels in *Lymnaea* neurons. *Am. J. Physiol.* **267**, C598–606 (1994).
17. Azizi, F., Matsumoto, P. S., Wu, D. X. & Widdicombe, J. H. Effects of hydrostatic pressure on permeability of airway epithelium. *Exp. Lung Res.* **23**, 257–267 (1997).
18. Kondo, M., Finkbeiner, W. E. & Widdicombe, J. H. Changes in permeability of dog tracheal epithelium in response to hydrostatic pressure. *Am. J. Physiol.* **262**, L176–182 (1992).
19. Clarke, L. L. A guide to Ussing chamber studies of mouse intestine. *Am. J. Physiol. Gastrointest. Liver Physiol.* **296**, G1151–1166 (2009).
20. Clarke, L. L. & Harline, M. C. CFTR is required for cAMP inhibition of intestinal Na+ absorption in a cystic fibrosis mouse model. *Am. J. Physiol.* **270**, G259–267 (1996).
21. Schultz, B. D., Singh, A. K., Devor, D. C. & Bridges, R. J. Pharmacology of CFTR chloride channel activity. *Physiol. Rev.* **79**, S109–144 (1999).
22. Flynn, A. N., Itani, O. A., Moninger, T. O. & Welsh, M. J. Acute regulation of tight junction ion selectivity in human airway epithelia. *Proc. Natl Acad. Sci. USA* **106**, 3591–3596 (2009).
23. Button, B. & Boucher, R. C. Role of mechanical stress in regulating airway surface hydration and mucus clearance rates. *Respir. Physiol. Neurobiol.* **163**, 189–201 (2008).
24. Fan, H. C., Zhang, X. & McNaughton, P. A. Activation of the TRPV4 ion channel is enhanced by phosphorylation. *J. Biol. Chem.* **284**, 27884–27891 (2009).
25. Hamill, O. P. & Martinac, B. Molecular basis of mechanotransduction in living cells. *Physiol. Rev.* **81**, 685–740 (2001).
26. van Doorninck, J. H. *et al.* A mouse model for the cystic fibrosis delta F508 mutation. *EMBO J.* **14**, 4403–4411 (1995).
27. Clarke, L. L. *et al.* Defective epithelial chloride transport in a gene-targeted mouse model of cystic fibrosis. *Science* **257**, 1125–1128 (1992).
28. Sukharev, S. & Anishkin, A. Mechanosensitive channels: what can we learn from 'simple' model systems? *Trends Neurosci.* **27**, 345–351 (2004).
29. Hale, T. *Exercise Physiology; A Thematic Approach.* (Wiley, New York; 2004).
30. Muhm, J. M. *et al.* Effect of aircraft-cabin altitude on passenger discomfort. *N. Engl. J. Med.* **357**, 18–27 (2007).
31. Furst, J. *et al.* Molecular and functional aspects of anionic channels activated during regulatory volume decrease in mammalian cells. *Pflugers Arch.* **444**, 1–25 (2002).
32. Sardini, A. *et al.* Cell volume regulation and swelling-activated chloride channels. *Biochim. Biophys. Acta* **1618**, 153–162 (2003).
33. Valverde, M. A. *et al.* Impaired cell volume regulation in intestinal crypt epithelia of cystic fibrosis mice. *Proc. Natl Acad. Sci. USA* **92**, 9038–9041 (1995).
34. Barriere, H. *et al.* CFTR null mutation altered cAMP-sensitive and swelling-activated Cl- currents in primary cultures of mouse nephron. *Am. J. Physiol.* **284**, F796–811 (2003).
35. Vazquez, E., Nobles, M. & Valverde, M. A. Defective regulatory volume decrease in human cystic fibrosis tracheal cells because of altered regulation of intermediate conductance Ca2+-dependent potassium channels. *Proc. Natl Acad. Sci. USA* **98**, 5329–5334 (2001).
36. Valverde, M. A. *et al.* Murine CFTR channel and its role in regulatory volume decrease of small intestine crypts. *Cell Physiol. Biochem* **10**, 321–328 (2000).
37. Belfodil, R. *et al.* CFTR-dependent and -independent swelling-activated K+ currents in primary cultures of mouse nephron. *Am. J. Physiol.* **284**, F812–828 (2003).

METHODS

Cell culture and *Cftr* knockout mice. Culturing of Calu-3 cells was as previously described in the patch-clamp[38] and Ussing chamber[39] studies. *Cftr* knockout mice (CFTR^{tm1Unc})[40] purchased from the Jackson Laboratory (Bar Harbor, Maine, USA) and their wild-type controls were reared for 2–3 months in the Laboratory Animal Service Center of the Chinese University of Hong Kong or in the Animal Care Facility of the Hong Kong University of Science and Technology before the experiments.

Patch-clamp recording. The experimental and data acquisition and analysis procedures were essentially the same as previously described[38]. In cell-attached recording, the pipette and bath solutions contained (in mM): 150 Tris-Cl, 2 $MgCl_2$, 1 $CaCl_2$, 5 HEPES, 30 sucrose, 10 D-glucose, pH 7.4 adjusted with Tris. In excised, inside-out recording, the pipette and bath solutions were 160 mM Tris-Cl and 30 mM sucrose (pH 7.0 adjusted with Tris). Negative pressures were applied to the back of the pipette manually through a 1-ml syringe attached to a three-way stopcock. The pressures were monitored by a pressure transducer (PM01R, World Precision Instruments) and the Axon pClamp9 software. The cAMP cocktail contained 10 μM forskolin, 200 μM cpt-cAMP and 100 μM IBMX.

The all-points amplitude histograms of traces in I–IV in Fig. 1a and Supplementary Fig. 1a were plotted from 2–3 s before (for baseline reference) and all data during the application of suction, and the ones of traces in V in Fig. 1a and Supplementary Fig. 1b were plotted from the entire trace.

Ussing chamber studies. The procedures for recording I_{sc} and I_{Cl} were basically the same as previously described[39] with some modifications. The mouse duodenum and jejunum were stripped from the muscular layer under a microscope and mounted on a homemade insert (area = 0.125 cm^2). The basolateral chamber was constantly gassed with 95% O_2 and 5% CO_2, as was the apical chamber except during the application of pressure. A brief pause (60–120 s) in the gassing in the apical chamber had no effect on the basal currents. Pressures were manually applied to the apical chamber through a homemade cap that sealed the chamber and was connected to a 10 ml syringe attached to a three-way stopcock, and the basolateral chamber was open to the atmosphere. The pressures were monitored through a pressure transducer (World Precision) by Axon MiniDigi 1A and AxoScope 9.0 software. The amplitudes of the pressure pulses for Calu-3 cells, mouse duodenum and jejunum were 5–60 mmHg, 40 mmHg and 30 mmHg, respectively; the durations of the pressure pulses for I_{sc} and I_{Cl} were 60 sec and 120 s, respectively; the pressure pulse was released at the response plateau in all the experiments. Test compounds were added only to the apical side in all experiments. In the mouse jejunum experiments, glucose in the mucosal bath solution was replaced by mannitol.

Statistics. Data are presented as means ± s.e.m. *P* values were determined using a two-tailed Student's *t*-test.

38. Wang, Y. *et al.* Regulation of CFTR channels by HCO(3)--sensitive soluble adenylyl cyclase in human airway epithelial cells. *Am. J. Physiol. Cell Physiol.* **289**, C1145–1151 (2005).
39. Wang, D., Sun, Y., Zhang, W. & Huang, P. Apical adenosine regulates basolateral Ca2+-activated potassium channels in human airway Calu-3 epithelial cells. *Am. J. Physiol. Cell Physiol.* **294**, C1443–1453 (2008).
40. Snouwaert, J. N. *et al.* An animal model for cystic fibrosis made by gene targeting. *Science* **257**, 1083–1088 (1992).

nature cell biology

DOI: 10.1038/ncb2053

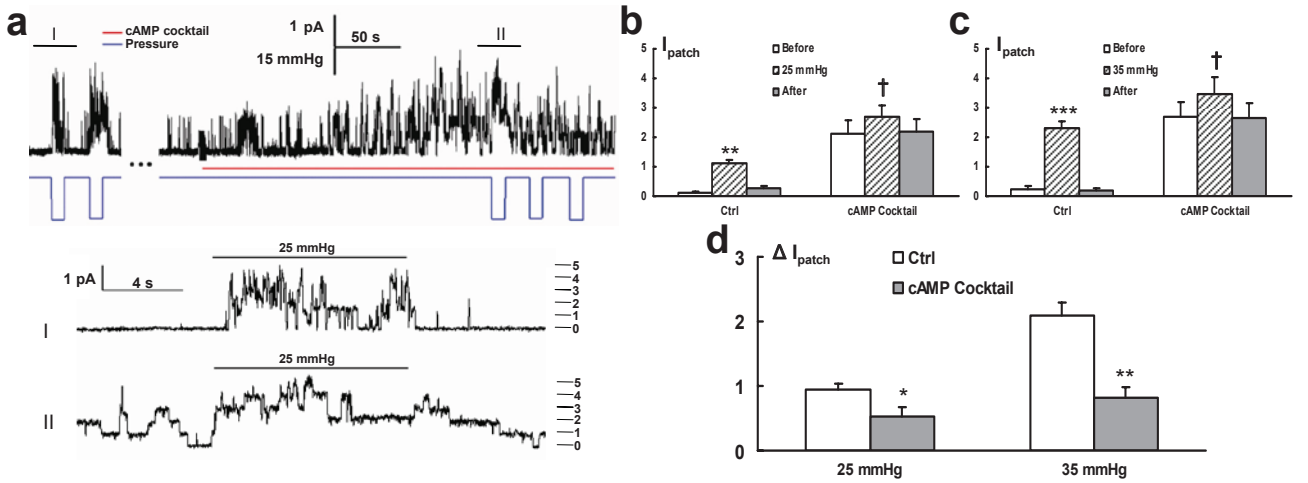

Figure S1 CFTR stretch-activation before and after cAMP activation in cell-attached membrane patches of Calu-3 cells. (**a**) Upper: CFTR in response to suction of 25 mmHg before and after cAMP. Dotted line, recording omitted for clarity. Lower: time-expansion of segments I-II. Numbers and dashes, the active channel number. **(b-c)** Summary data of CFTR channel activity in response to suction of 25 (**b**) and 35 (c) mmHg before and after cAMP. CFTR channel activity is presented as the patch current (I_{patch}) in lieu of NPo, the calculation of which is complicated by the different unitary conductances of stretch- and cAMP-activated CFTR channels in these experiments (see Fig. 2 and the text). **, different from before suction, $P = 0.0051$, ***, $P = 0.00079$, †, $P \geq 0.36$, data are mean ± s.e.m. of $n = 7$ patches. (**d**) Summary data of I_{patch} change (ΔI_{patch}) in **b-c**. ΔI_{patch} is the difference between I_{patch} during (10 s) and before (10 s) suction in **b** and **c**. *, different from before cAMP, $P = 0.039$, **, $P = 0.0035$.

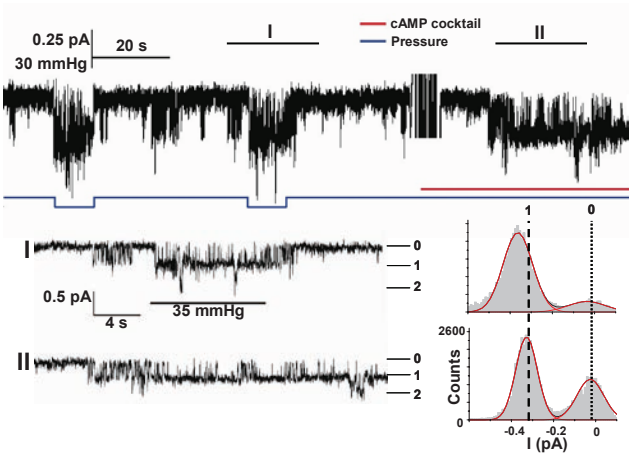

Figure S2 CFTR stretch-activation at a positive Vp in a cell-attached membrane patch of Calu-3 cells. Upper: a trace of CFTR single channels in response to suction and cAMP at +100 mV Vp. Lower: time-expanded traces of the segments a-b and their corresponding all-points amplitude histograms of the first-level channel. Note the shift of the current amplitude of the first-level channel in response to suction, compared to that in response to cAMP, in the all-points amplitude histograms.

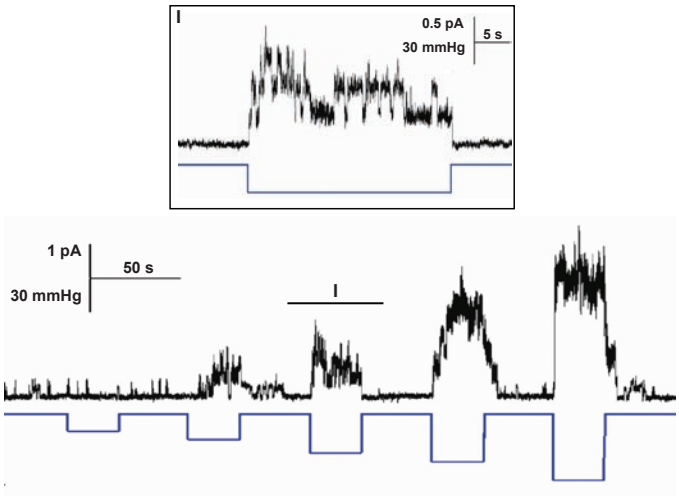

Figure S3 Dose response of CFTR channels to pressures in cell-attached membrane patches of Calu-3 cells. Shown is a representative trace of CFTR channels in response to suctions ranging from 15 to 60 mmHg at -60 mV Vp in a cell-attached membrane patch which contained multiple channels. Inset, the magnification of segment I.

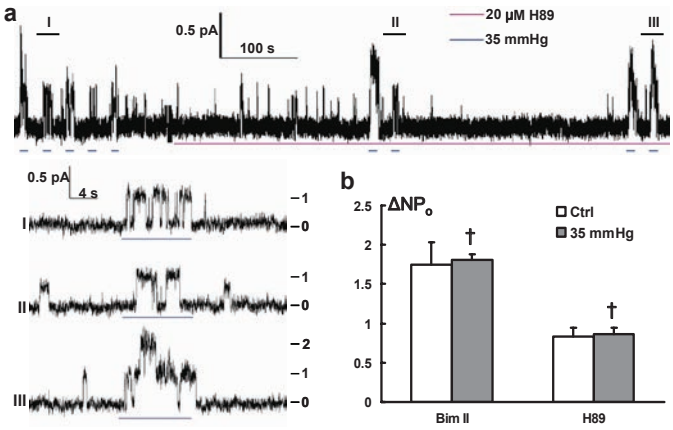

Figure S4 Stretch activation of CFTR before and after PKA and PKC blockers in cell-attached membrane patches of Calu-3 cells. (**a**) Upper: CFTR in response to suction of 35 mmHg before and after 20 μM H89, a PKA blocker. Lower: time-expansion of segments I-III. Numbers and dashes, the active channel number. **(b)** Summary data of CFTR NPo change (ΔNPo) before and after 20 μM H89, a PKA blocker, or 4 μM BIMII, a PKC blocker. ΔNPo is the difference between NPo during (10 s) and average NPo of before (10 s) and after (10 s) suction. †, $P \geq 0.81$. $n = 3$ patches for both H89 and BIMII. All data in S-Fig. 4 are mean ± s.e.m.

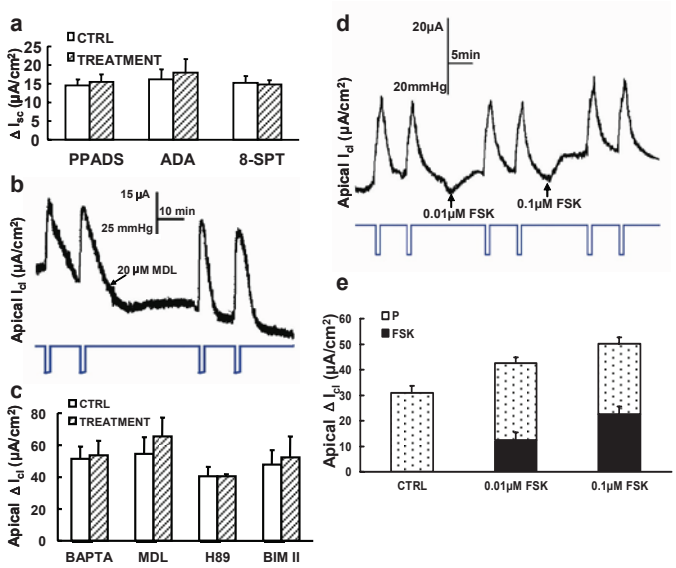

Figure S5 The stretch response of Calu-3 monolayers is not mediated by PKA and PKC signaling. **(a)** Summary data of the effect of PPADS (50 μM, n = 4), adenosine deaminase (ADA, 1U/ml, n = 4), and 8-SPT (20 μM, n = 4) on stretch-activated ΔIsc**. (b)** Representative trace of stretch-activated ΔI_{Cl} before and after 20 μM MDL-12330A. **(c)** Summary data of **b** (n = 7), and similar experiments with BAPTA-AM (50 μM, n = 4), H89 (20 μM, n = 3), or BIMII (4 μM, n = 4). (**d**) Stretch-activated apical ΔI_{Cl} before and after 0.01 and 0.1 μM forskolin. (**e**) Summary data of **d** (n = 6). All data in S-Fig. 5 are mean ± s.e.m.

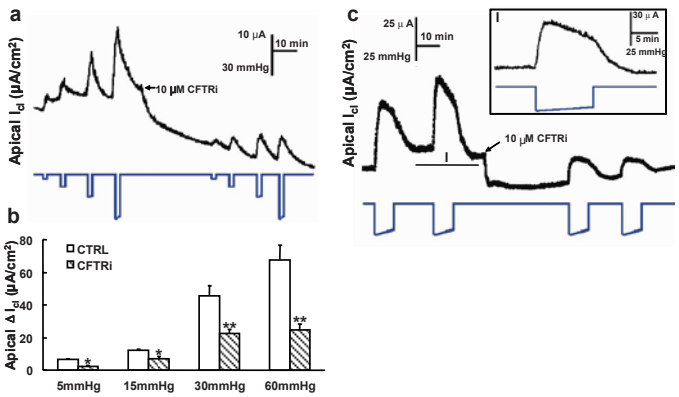

Figure S6 Characterization of stretch-activated ΔI_{Cl} in Calu-3 cells. **(a)** Representative trace of ΔI_{Cl} in response to increasing apical suctions before and after 10 μM CFTRi. **(b)** Summary data of **a** ($n = 4$). *, different from control, $P \leq 0.035$; **, $P \leq 0.007$. **(c)** Representative trace of ΔI_{Cl} in response to a prolonged stretch ($n = 3$). Inset, time expansion of segment I. All data in S-Fig. 6 are mean ± s.e.m.